

et des Molecules, edited by R. Lefebvre and C. Moser (Editions du Centre National de la Recherche Scientifique, Paris, 1967), p. 311.

⁴H. F. Schaefer III, R. A. Klemm, and F. E. Harris, *Phys. Rev.* **176**, 49 (1968).

⁵K. A. Brueckner, *Phys. Rev.* **97**, 1353 (1955); **100**, 36 (1955); *The Many-Body Problem* (John Wiley & Sons, Inc., New York, 1959).

⁶J. Goldstone, *Proc. Roy. Soc. (London)* **A239**, 267 (1957).

⁷H. P. Kelly, *Phys. Rev.* **173**, 142 (1968).

⁸P. G. H. Sandars, in *La Structure Hyperfine des Atomes et des Molecules*, edited by R. Lefebvre and C. Moser (Editions du Centre National de la Recherche Scientifique, Paris, 1967), p. 111; *Advan. Chem. Phys.* (to be published).

⁹H. P. Kelly, *Phys. Rev.* **131**, 684 (1963).

¹⁰H. P. Kelly, *Phys. Rev.* **136**, B896 (1964).

¹¹H. P. Kelly, *Phys. Rev.* **144**, 39 (1966).

¹²E. S. Chang, R. T. Pu, and T. P. Das, *Phys. Rev.*

174, 1 (1968).

¹³J. D. Lyons, R. T. Pu, and T. P. Das, to be published.

¹⁴R. E. Trees, *Phys. Rev.* **92**, 308 (1953).

¹⁵A. R. Edmonds, *Angular Momentum in Quantum Mechanics* (Princeton University Press, Princeton, New Jersey, 1960), p. 118.

¹⁶H. Kopfermann, *Nuclear Moments* (Academic Press, Inc., New York, 1958).

¹⁷E. D. Commins and H. R. Feldman, *Phys. Rev.* **131**, 700 (1963).

¹⁸G. H. Fuller and V. W. Cohen, *Nuclear Data Sheets*, compiled by K. Way *et al.* (Printing and Publishing Office, National Academy of Sciences - National Research Council, Washington 25, D.C.), Appendix I.

¹⁹M. J. Stevenson and C. H. Townes, *Phys. Rev.* **107**, 635 (1957).

²⁰R. A. Kamper, K. R. Lea, and C. D. Lustig, *Proc. Phys. Soc.* **70B**, 897 (1957).

²¹R. M. Sternheimer, *Phys. Rev.* **86**, 316 (1952).

Intensity and Gain Measurements on the Stimulated Raman Emission in Liquid O₂ and N₂ †

J. B. Grun,* A. K. McQuillan, ‡ and B. P. Stoicheff
Department of Physics, University of Toronto, Toronto 5, Canada
 (Received 25 November 1968)

In liquid O₂ and N₂ the threshold for stimulated Raman emission is found to be much lower than for other nonlinear processes. Thus it is possible to make reliable measurements of the intensity of Raman emission over a large range of incident laser power by using a simple longitudinal geometry. Several distinct regions of emission were investigated, including normal Raman scattering, exponential gain, onset of oscillation, and saturation. There is good agreement with theory.

INTRODUCTION

It is well known¹⁻³ that the comparison of theoretical and experimental values of intensity and gain in stimulated Raman emission is complicated by several competing processes such as self-focusing, and Brillouin and Rayleigh scattering, all of which may have similar appearance thresholds. Thus, anomalous intensity behavior in many liquids and even in gases⁴⁻⁶ and solids⁷ appears to be the rule rather than the exception. One important consequence is that the premature onset of oscillation has precluded the observation of the expected exponential gain in most materials, with the exception of gaseous hydrogen, liquid

acetone, and carbon tetrachloride.⁸ Bloembergen and Lallemand^{3,6} have overcome some of these difficulties by the use of a Raman amplifier and have demonstrated its importance in obtaining reliable values of the Raman gain. Other useful experimental arrangements in such studies include the transverse resonator of Dennis and Tannenwald,⁴ the off-axis resonator of Jennings and Takuma,¹⁰ and the diffusely pumped amplifier of Bortfeld and Sooy.¹¹ More recently, Shapiro, Giordmaine, and Wecht,¹² Bret and Weber,¹³ and Kaiser and Maier¹⁴ have shown that with picosecond and subnanosecond laser pulses stimulated Raman scattering is the dominant nonlinear scattering process in several liquids, and thus have obtained good agreement

with theoretical intensities.

The present investigation of laser stimulated Raman emission from liquid O_2 and N_2 arose from the results of earlier studies of the spectra of the normal and stimulated scattering. In one, it was shown that the linewidth of the normal Raman scattering was exceptionally narrow indicating a large Raman gain¹⁵; in another, concerning the stimulated Raman emission, extremely sharp spectral lines were observed (Fig. 1) without any evidence of broadening,¹⁶ thus indicating that self-focusing and other scattering processes were not prominent. From these results we concluded that possibly the threshold for stimulated Raman scattering is lower than for the competing processes, in which case liquid O_2 and N_2 would be ideal substances for experimental study. Indeed, the present investigation has shown that liquid O_2 and N_2 are unique in this respect and no self-focusing or stimulated Brillouin scattering has been detected up to the highest incident laser power.

We wish to report our observations of the intensity of Raman Stokes radiation corresponding to the vibrational frequencies 1552.0 cm^{-1} and 2326.5 cm^{-1} of liquid O_2 and N_2 , respectively. A simple longitudinal arrangement was used. The range of Raman intensity measurements includes the normal emission which varies linearly with incident laser power, a region of exponential gain over several orders of magnitude, the onset of oscillation with feedback by Rayleigh scattering and finally a region of saturation and depletion. The observed gain is in good agreement with that calculated from our experimentally determined cross-section for scattering.

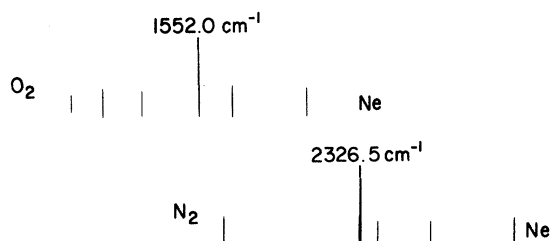


FIG. 1. Stimulated Raman spectra of liquid O_2 and N_2 showing the first-order Stokes vibrational lines at 1552.0 and 2326.5 cm^{-1} , respectively. The resolving power of the grating spectrograph is 10^5 .

APPARATUS AND EXPERIMENTAL PROCEDURE

The exciting source was a giant-pulse ruby laser with a rotating prism at one end, and at the other a plane parallel reflector ($\sim 25\%$ reflectivity) of Corning 2-58 glass which served as a mode selector¹⁶ and also as a filter. The radiation was emitted in a single pulse of ~ 30 -nsec duration and

in a single (or nearly single) axial mode. Good reproducibility in the laser pulse was obtained by firing the laser at constant power near threshold, at regular (3 min) intervals with the ruby at a constant temperature (-10°C). This procedure also eliminated any spatial drift of the laser beam at the distant spectrometer slit.

The temporal behavior of a typical laser pulse is shown in Fig. 2(a). A study of the spatial intensity distribution of the laser beam was made at a magnification of $20\times$ and by photographing the beam after attenuation by neutral density filters. This showed the presence of several intensity maxima [Fig. 3(a)] which increased the effective intensity of the laser beam to twice the average intensity. Also, the laser radiation was found to be plane polarized to better than 2000:1.

The longitudinal arrangement shown in Fig. 4 was used for the measurements of Raman scattering intensity and state of polarization in the forward direction. The sample container was a simple Dewar of 1 liter capacity with a path length of 5.8 cm between the two inner windows. It was positioned approximately 4 m from the laser in order to reduce possible feedback of scattered radiation to the laser. At each filling of the Dewar, the liquid was passed through a 5μ millipore filter to remove any dust particles. A short time after a filling, the liquid became quiescent.

In order to increase the laser power density incident on the samples, the beam diameter was

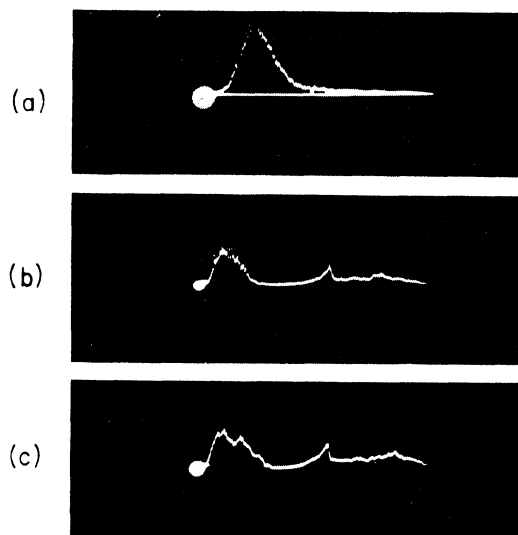


FIG. 2. (a) Typical laser pulse monitored with an ITT FW114A photodiode, and displayed on a Tektronix 519 oscilloscope. (b) Typical first-order Stokes pulse obtained in the saturation region, and the corresponding depleted laser pulse at the right. (c) Same as (b), but with the Stokes pulse also showing some depletion at higher laser power.

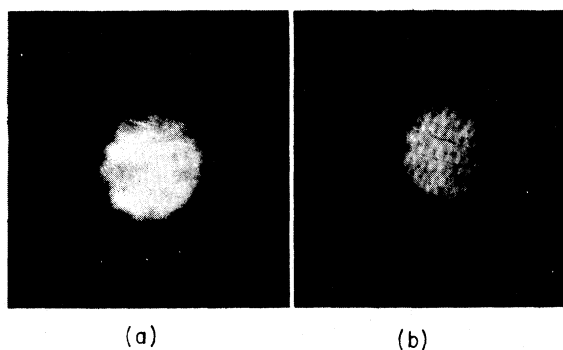


FIG. 3. Near-field patterns showing the spatial intensity distribution of the incident laser beam (a) and the first Stokes emission (b), magnified 20 \times . Mottled appearance of Stokes picture is caused by laser attenuating filters.

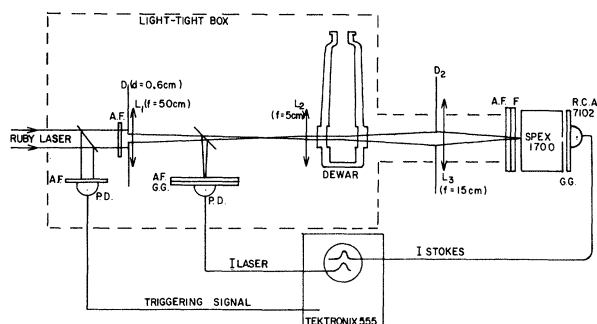


FIG. 4. Diagram of apparatus used for Raman intensity measurements. Explanation of symbols: *D* - diaphragm, *A. F.* - attenuating filter, *G. G.* - ground glass, *P. D.* - E. G. & G photodiode (SGD-100), *L* - lens, *F* - filter.

reduced by a factor of about 10 (to 0.6 mm) with a system of two lenses. The incident laser power was varied from 30 kW to 600 kW by inserting calibrated neutral density filters of glass in the beam at the entrance diaphragm *D*₁ and lens *L*₁. The laser pulse was monitored with an EG & G photodiode (SGD-100), and displayed on a Tektronix 555 (or 519) oscilloscope. An essentially parallel laser beam was incident on the sample. The radiation scattered in the forward direction was collected through the exit diaphragm *D*₂ and focused on the slit of the spectrometer. The laser light entering the spectrometer was attenuated with calibrated filters. A grating spectrometer (Spex 1700) having a dispersion of 10 Å/mm was used with both entrance and exit slits open to 3 mm. Measurements of Stokes intensities were made with an RCA 7102 Photomultiplier having a cooled photocathode (-10°C). The signal was amplified 40 times by a two-stage emitter follower,

and fed into a type *L* preamplifier of the oscilloscope. The pulse heights from the oscilloscope traces gave an effective measurement of the intensity of Stokes emission during each laser pulse. Brief studies of the laser and Stokes pulse envelopes were made with a fast photodiode (ITT FW 114A) and a Tektronix 519 oscilloscope. Depolarization measurements were carried out with a Nicol prism placed at the slit of the spectrometer.

Several precautions were taken to reduce any stray light and to minimize its effect on the intensity measurements, especially of the low-intensity normal Raman scattering. The main sources of unwanted stray light were found to be the laser flashlamp, and optical filters and lenses of glass along the laser beam which emitted relatively intense fluorescence radiation. Thus, all of the optics and sample Dewar were enclosed in a light-tight box having a 6 mm entrance aperture; diaphragms were placed along the laser beam path in front of lenses; and quartz lenses were used instead of glass lenses to minimize the fluorescence. Finally, the effects of the broad band fluorescence were suppressed by the use of a high-dispersion spectrometer.

For each liquid, the intensity measurements were carried out in two stages. In the low-intensity region of the normal Raman scattering, the light-collecting cone was 1.45×10^{-3} sr for N₂ and 5.80×10^{-4} sr for O₂. Calibrated filters were inserted in front of the spectrometer slit to cover the intensity range. In the high-intensity region of stimulated Raman emission the light-collecting cone was smaller, being 1.30×10^{-4} sr for both N₂ and O₂. Again, calibrated filters were used to make intensity measurements over approximately ten orders of magnitude. The laser pulse energy was measured with a calibrated thermopile (TRG 100). The many optical filters used to attenuate the laser and Raman radiation were calibrated spectrophotometrically (Beckman DU) each to an accuracy of 3%. The transmission characteristics of the spectrometer and the sensitivity of the photomultiplier were measured over the required wavelength region (and for light of parallel and perpendicular polarization) using a NBS standard lamp.

An estimate of the possible errors in making absolute intensity measurements of the Raman scattering indicated an accuracy of $\pm 50\%$, the main source of error arising from the many filters used in attenuating the laser radiation. However the accuracy of relative intensity measurements was considered to be better than $\pm 30\%$.

BRIEF RÉSUMÉ OF THEORY

The theory of stimulated Raman scattering has been developed by many authors, notably, Hellwarth,¹⁷ Bloembergen and Shen,¹⁸ Townes and co-workers,¹⁹ and Maker and Terhune.²⁰ They have

shown that the stimulated Stokes emission grows exponentially from noise according to the relation

$$I_S(l) = I_S(0)e^{+gIl_0}. \quad (1)$$

Here, $I_S(l)$ is the intensity of the stimulated Stokes emission, $I_S(0)$ is the intensity of the normal (spontaneous) Stokes emission, I_0 is the incident laser power density, and l is the length of the amplifying medium. The gain g is given by

$$g = \frac{2c^2}{\pi\hbar n^2} \frac{N}{\Delta\nu(\nu_0 - \nu_R)^3} d\sigma_{11}/d\Omega. \quad (2)$$

In general, and in the present work, g represents the gain for radiation polarized in the same plane as the incident plane-polarized laser radiation. In Eq. (2), c is the velocity of light, \hbar is Planck's constant, n the refractive index, N is the effective number of molecules per cm^3 , $\Delta\nu$ is the normal Raman linewidth, $\nu_0 - \nu_R$ is the frequency of the Raman line. The quantity $d\sigma_{11}/d\Omega$ is the total differential cross-section per molecule per sr for the one polarization, and may be evaluated from an absolute-intensity measurement of normal Raman scattering. Such a measurement gives the total differential cross-section for both polarized and depolarized scattering defined by²¹

$$\frac{d\sigma}{d\Omega} = \frac{2^4\pi^4}{c^4} \left(\frac{\hbar}{8\pi^2\nu_R} \right) \frac{d}{\mu} (\nu_0 - \nu_R)^4 K \left(\frac{45\alpha'^2 + 7\gamma'^2}{45} \right) \quad (3)$$

for plane-polarized light incident on a system of randomly oriented molecules and observation in the scattering plane. Here ν_R is the frequency of the Raman-active molecular vibration, d is the degree of degeneracy of the vibration (=1 for the totally symmetric vibrations), μ is the reduced mass, and α' and γ' are, respectively, the isotropic and anisotropic parts of the derivative of the polarizability with respect to the internuclear coordinate at the equilibrium position. The constant K is the local field correction given by²²

$$K = (n_s/n_0)(n_s^2 + 2)^2(n_0^2 + 2)^2/81, \quad (4)$$

where n_0 and n_s are the indices of refraction at the laser and Stokes frequencies, respectively. In order to evaluate γ' and α' , it is necessary to measure the depolarization ratio

$$\rho = I_{\perp}/I_{\parallel} = 3\gamma'^2/(45\alpha'^2 + 4\gamma'^2).$$

Here I_{\perp} and I_{\parallel} are the intensities of scattered light polarized \perp and \parallel , respectively, to the plane-polarized incident light.

It may be mentioned that Eq. (3) is valid only when the frequency of the incident exciting light is far from the main absorption bands of O_2 and N_2 which occur in the vacuum ultraviolet region.

EXPERIMENTAL RESULTS AND DISCUSSION

The observed intensity of first-order Stokes radiation over a range of incident laser intensity is shown in Fig. 5 for liquid O_2 and in Fig. 6 for liquid N_2 . For both liquids, it was possible to investigate the Raman intensity over a range of approximately 12 orders of magnitude, from the very low intensity of normal scattering through a region of exponential amplification and oscillation to an intensity approaching the incident intensity, and finally saturation. These results will be discussed below under the headings (a) normal Raman scattering, (b) exponential gain, and (c) oscillation and saturation.

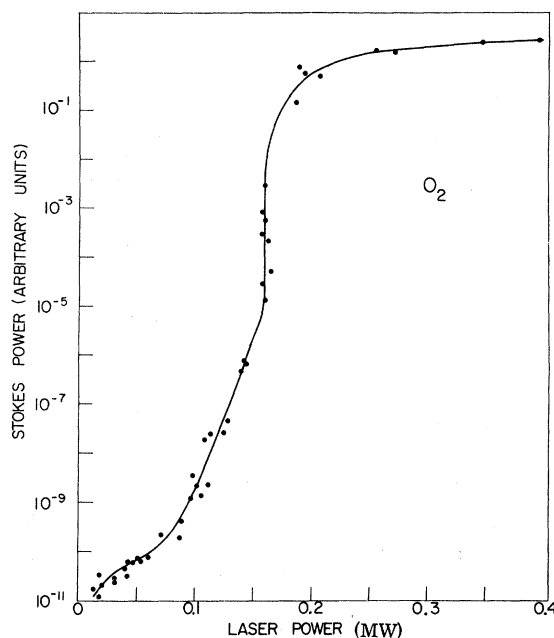


FIG. 5. Experimental curve for liquid oxygen showing Raman Stokes power as a function of incident ruby laser power.

(a) Normal Raman Scattering

The region of normal Raman scattering is one of very low intensity. Our measurements for O_2 and N_2 are given in Fig. 7. Although the data show considerable scatter, it is seen that there is a linear dependence of Raman intensity on incident laser intensity, as expected from theory. The slopes of the graphs of Fig. 7 were used to determine values of the differential scattering cross-section.

As already mentioned, the errors in making these absolute intensity measurements are approximately $\pm 50\%$, whereas the accuracy of the relative measurements is perhaps $\pm 30\%$. Thus the present

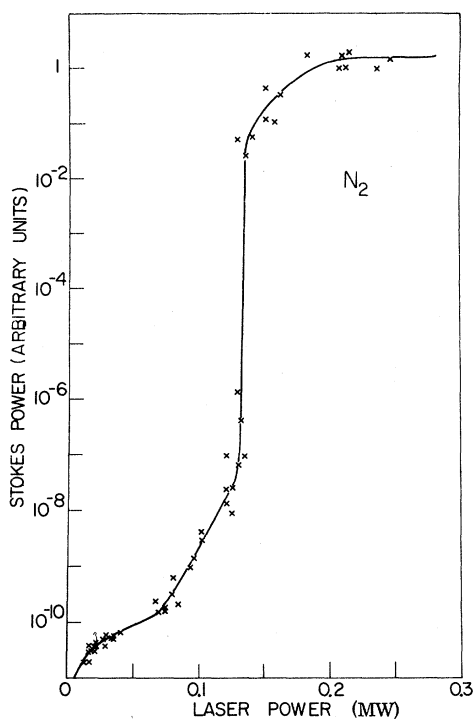


FIG. 6. Experimental curve for liquid nitrogen showing Raman Stokes output power as a function of incident ruby laser power.

TABLE I. Values of the total differential scattering cross-section for the 992 cm⁻¹ Raman radiation of liquid benzene.

Authors	$\frac{d\sigma}{d\Omega}$ (10 ⁻³⁰ cm ² sr ⁻¹)	$\frac{d\sigma}{d\Omega}$ corrected for 6943 Å (10 ⁻³⁰ cm ² sr ⁻¹) ^a
Damen, Leite, and Porto ²³	6.7 ± 1.2 (6328 Å)	4.5 ^a
Skinner and Nilsen ²⁴	37.5 ± 4 (4880 Å)	4.95 ^b
McClung and Weiner ²²	5.9 ± 3 (6943 Å)	5.9
Bret <i>et al.</i> ²	9 (6943 Å)	9
Present authors	6.6 ± 3 (6943 Å)	6.6

^aCalculated from $I\alpha(\nu - \nu_v)^4$, since the frequency of the exciting radiation ν is far from principal absorption frequencies. The Raman vibrational frequency is ν_v .

^bCalculated from $I\alpha(\nu - \nu_v)^4/(\nu_a - \nu)^2$, since the frequency of the exciting radiation is near an absorption frequency ν_a .

method of determining the absolute Raman intensities was checked by measuring the scattering for the 992-cm⁻¹ line of liquid benzene, and com-

paring the resultant value of the total differential scattering cross-section $d\sigma/d\Omega$ with values measured by other experimenters. This cross-section is related to experimentally measurable quantities by the equation

$$d\sigma/d\Omega = P_R/P_0 N l \Omega.$$

Here, P_R is the Raman power for the whole line scattered into the solid angle Ω and P_0 is the corresponding laser power, N is the density of molecules per cm³ in the scattering medium, and l is the path length ($l = 10$ cm in our C₆H₆ experiment). Some of the recent values of $d\sigma/d\Omega$, for benzene are shown in Table I along with our value of $6.6 \pm 3 \times 10^{-30}$ cm² per molecule per sr. It is seen that the most accurate values are those obtained by Damen, Leite, and Porto²³ with a He-Ne laser and by Skinner and Nilsen²⁴ with an Ar⁺ laser, which after correction for the ν^4 frequency dependence, are in very good agreement. We

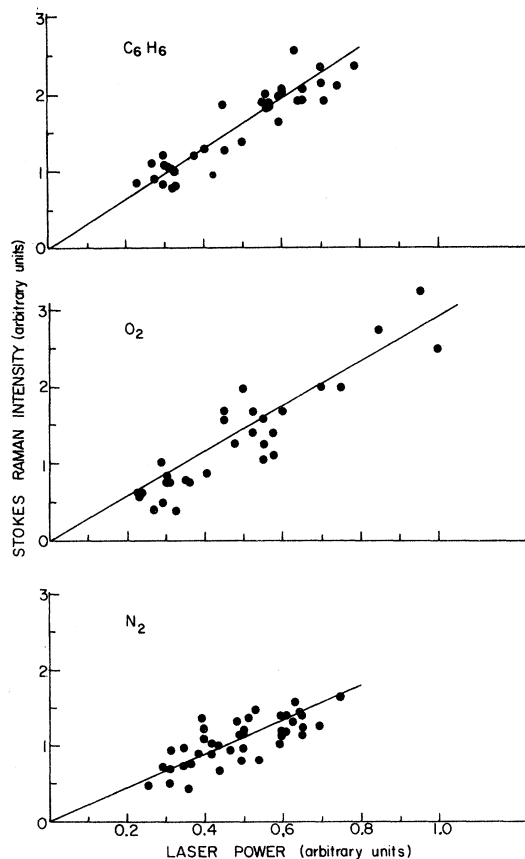


FIG. 7. Experimental measurements of normal Raman scattering for liquids, benzene, oxygen, and nitrogen. (Experimental scatter results from very low light levels used, necessitating a high amplification of the photo-multiplier signal.)

have therefore taken the value $d\sigma/d\Omega = 4.50 \times 10^{-30}$ cm² for benzene (at $\lambda = 6943$ Å) as a basis for σ r evaluations, and have measured the ratio of the Raman intensities of the 2326-cm⁻¹ line for N₂ and 1552-cm⁻¹ line for O₂ relative to the 992 cm⁻¹ for C₆H₆.

The results of these intensity measurements are given in Table II along with measurements of the depolarization ratio ρ for liquid O₂ and N₂. (We have also included values obtained for liquid CS₂.) The measured values of $d\sigma/d\Omega$ and of ρ were used to calculate values of $\alpha' = d\alpha/dr$, the rate of change of polarizability with nuclear displacement, from Eq. (3), after applying the local field correction K [Eq. (4)]. These are included in Table II. The values $\alpha' = 1.6 \times 10^{-16}$ cm² and 1.35×10^{-16} cm² for liquid N₂ and O₂, respectively, are the same as the values obtained for gaseous N₂ and O₂ by Stansbury, Crawford, and Welsh.²⁵ Our measured value of ρ for liquid N₂ agrees with that measured in the gas by Cabannes and Rousset,²⁶ but our value of ρ for O₂ is considerably lower than theirs.

(b) Exponential Gain

Under the present experimental conditions, the region of normal Raman scattering appears to hold up to incident laser powers of ~ 70 kW. At higher laser powers, both liquids exhibit regions of exponential gain, as shown by the linear portions of the graphs (plotted on semilog scales) in Figs. 5 and 6. For N₂ this region extends over a range

of three orders of magnitude and for O₂, four orders of magnitude of Stokes amplification. These results represent stable regions of gain up to factors of at least e^6 and e^8 for liquid N₂ and O₂, respectively.

Values of the gain $g(\text{exp})$ were obtained from the slopes of the linear portions of the intensity curves (Figs. 5 and 6). These are given in Table III. Also listed for comparison are calculated values of the gain $g(\text{calc})$. The calculated values are based on the scattering cross-section $d\sigma/d\Omega$ evaluated here and on the linewidths 0.067 cm⁻¹ for N₂ and 0.117 cm⁻¹ for O₂ measured by Clements and Stoicheff,¹⁵ making use of Eq. (2). It is seen that the values $g(\text{exp})$ and $g(\text{calc})$ are in good agreement.

(c) Oscillation and Saturation

For both liquids, the regions of exponential gain are abruptly terminated as shown by the discontinuity in slope of the Stokes intensity curves Figs. 5 and 6. These sharp changes in slope represent the onset of Raman oscillation with a rapid rise in output power. The oscillation threshold for N₂ occurs at somewhat lower laser power than for O₂; 0.13 MW compared with 0.16 MW for O₂. These values were not significantly affected by tilting the Dewar with respect to the incident laser beam or by the presence of ice particles in the liquids (although in the latter case the experimental error was greatly increased). The onset of oscillation is therefore not considered to arise from reflection at the windows or from scattering by

TABLE II. Values of the total differential cross-section, derivative of the polarizability and depolarization ratio.

Liquid	ν_{ν} (cm ⁻¹)	$\frac{(d\sigma/d\Omega)_{\text{Liquid}}}{(d\sigma/d\Omega)_{\text{C}_6\text{H}_6}}$	$d\sigma/d\Omega$ (10 ⁻³⁰ cm ² sr ⁻¹)	α' (10 ⁻¹⁶ cm ²)	ρ
O ₂	1552.0	0.056 ± 0.017	0.250 ± 0.075	1.35 (1.4) ^b	0.11 ± 0.01
N ₂	2326.5	0.041 ± 0.012	0.185 ± 0.055	1.60 (1.6) ^b	0.10 ± 0.01
C ₆ H ₆	992.2	1.00	4.5 ^a	2.84	...
CS ₂	655.6	2.03 ± 0.60	9.1 ± 2.7	2.91	0.17 ± 0.02

^aValue of Damen, Leite, and Porto²³ corrected for 6943 Å radiation.

^bValues given by Stansbury, Crawford, and Welsh²⁵ for gaseous O₂, N₂.

TABLE III. Values of the Raman gain.

Liquid	$Nd\sigma_{\parallel}/d\Omega$ (10 ⁻⁸ cm ⁻¹ sr ⁻¹)	$\Delta\nu^a$ (cm ⁻¹)	$g(\text{calc})$ (10 ⁻² cm MW ⁻¹)	$g(\text{exp})$ (10 ⁻² cm MW ⁻¹)
O ₂	0.48 ± 0.14	0.117	1.45 ± 0.4	1.60 ± 0.50
N ₂	0.29 ± 0.09	0.067	1.70 ± 0.5	1.60 ± 0.55
C ₆ H ₆	3.06	2.15	0.28	...
CS ₂	7.55	0.50	2.4	...

^aValues of linewidths measured by Clements and Stoicheff.¹⁵

bubbles, dust, or ice particles. Also, we have experimentally ruled out the possibility that the rapid rise in output power is caused by self-focusing. Near-field photographs of the laser and Stokes radiation at the exit window show no evidence of filament formation and uniform Stokes emission over the beam cross-section [Fig. 3(b)]. No filaments were observed up to the highest laser power used 1 MW, where the self-focusing length is calculated to be 5 cm for O₂ and 9 cm for N₂. The critical power for self-focusing^{27,28} calculated from the known Kerr constants²⁹ is 200 kW for O₂ and 600 kW for N₂. The observed onset of oscillation occurs at lower laser powers as mentioned above. Moreover, the ratio of laser power at threshold of oscillation in O₂ to that in N₂ was measured to be 1.20 ± 0.006 as compared with the ratio of 0.3 for the respective critical powers for self-focusing.

We believe that the most likely cause of oscillation is feedback of Stokes radiation scattered in the backward direction by Rayleigh scattering. This is suggested by the high Raman gain for these liquids and by the ratio of 1.2 for the gain constants of O₂ and N₂, which is the same value as the ratio of laser power for oscillation. The Rayleigh scattering intensity determined by Stansbury, Crawford, and Welsh²⁵ for gaseous O₂ and N₂, together with the local field factor for the liquids, leads to a feedback factor of $Nd\sigma/d\Omega$ (Rayleigh) = 6.1×10^{-6} per cm per unit solid angle for liquid N₂ and 6.6×10^{-6} units for O₂. For the effective solid angle of our experiments ($\sim 10^{-4}$ sr) the feedback factor is approximately 10^{-9} per cm, which is sufficient to explain the onset of oscillation.

In the region of oscillation the rise in Stokes intensity is very steep, and represents an increase of five orders of magnitude for liquid O₂ and seven orders of magnitude for liquid N₂.^{6,30} The uppermost portions of the intensity curves (Figs. 5 and 6) are similar, and indicate strong depletion of laser radiation and conversion to Stokes radiation. The oscilloscope trace in Fig. 2(b) shows a typical pulse of Stokes radiation in this region with the corresponding laser pulse severely distorted. This process results in the flat tops of the intensity curves and is the region of saturation. At still higher incident laser powers, the first-order Stokes radiation is converted to second-order Stokes (and anti-Stokes radiation) which results in depletion of the first-order Stokes intensity. This depletion is shown in the oscilloscope trace of Fig. 2(c).

A brief study of the conversion of laser radiation to first-order Stokes radiation for liquid N₂ was carried out, and the results are presented

in Fig. 8. Here is plotted the ratio P_{out}/P_{in} , normalized for the laser radiation. The general behavior of this ratio is in good agreement with the theory of Shen and Bloembergen.¹⁸ Figure 8 shows high conversion of approximately 75% laser radiation to first-order Stokes radiation in the saturation region.

CONCLUSION

This experiment has shown that liquid N₂ and O₂ are important materials for the study of stimulated Raman scattering. Because of their high Raman gain, the stimulated Raman effect emerges as the dominant nonlinear process in these liquids. Thus it was possible to investigate the intensity characteristics and build-up of Stokes radiation over a range of 12 orders of magnitude; from the low-intensity normal scattering through exponential amplification, oscillation and saturation, and eventual depletion. A detailed study of the region of normal scattering and exponential gain shows very good agreement with theory. The regions of higher intensity also reveal the expected theoretical behavior and warrant closer study. Finally, the high conversion efficiency of laser to Raman Stokes radiation indicates that these liquids are very useful as new frequency sources.

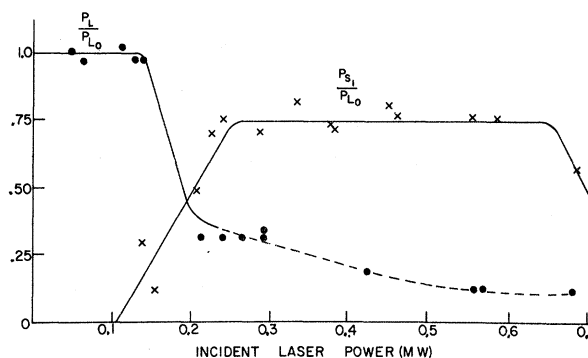


FIG. 8. Experimental curves showing how the ratios of the laser power (P_L) and the first Stokes power (P_S) at the exit of the Dewar, to the incident laser power (P_{L0}), vary with the incident laser power. The dashed curve in the depleted laser region is only approximate as the laser pulse was severely distorted.

ACKNOWLEDGMENT

We are very grateful to Dr. Fujio Shimizu for many helpful discussions.

† This research is part of Project DEFENDER under the joint sponsorship of the Advanced Research Projects Agency, the U. S. Office of Naval Research, and the Department of Defense. Also supported by the National Research Council, Canada, and the University of Toronto.

* On leave from Laboratoire de Spectroscopie, Université de Strasbourg, France.

‡ Holder of Province of Ontario Government Scholarships 1965-68.

¹J. F. McClung, W. G. Wagner, and D. Weiner, *Phys. Rev. Letters* **15**, 96 (1965); in *Physics of Quantum Electronics*, edited by P. L. Kelley, B. Lax, and P. E. Tannenwald (McGraw-Hill Book Company, Inc., New York, 1966), pp. 155-158.

²G. Bret, *Compt. Rend.* **259**, 2991 (1964); **260**, 6323 (1965); G. Bret and G. Mayer, in *Physics of Quantum Electronics*, edited by P. L. Kelley, B. Lax, and P. E. Tannenwald (McGraw-Hill Book Company, Inc., New York, 1966), pp. 180-191; G. Bisson, G. Bret, M. Denariez, F. Gires, G. Mayer, and M. Paillette, *J. Chim. Phys. (Paris)* **64**, 197 (1967).

³P. Lallemand and N. Bloembergen, *Appl. Phys. Letters* **6**, 210, 212 (1965); in *Physics of Quantum Electronics* edited by P. L. Kelley, B. Lax, and P. E. Tannenwald (McGraw-Hill Book Company, Inc., New York, 1966), pp. 137-154.

⁴R. W. Minck, E. E. Hagenlocker, and W. G. Rado, *Phys. Rev. Letters* **17**, 229 (1966).

⁵G. Bret and M. Denariez, *Phys. Letters* **22**, 583 (1966).

⁶N. Bloembergen, G. Bret, P. Lallemand, A. Pine, and P. Simova, *IEEE J. Quantum Electron.* **QE-3**, 197 (1967).

⁷G. Bisson and G. Mayer, *J. Phys.* **29**, 97 (1968).

⁸G. Bret and M. Denariez, *J. Chim. Phys. (Paris)* **64**, 222 (1967).

⁹J. H. Dennis and P. E. Tannenwald, *Appl. Phys. Letters* **5**, 58 (1964).

¹⁰D. A. Jennings and H. Takuma, *Appl. Phys. Letters* **5**, 239 (1964).

¹¹D. P. Bortfeld and W. R. Sooy, *Appl. Phys. Letters* **7**, 283 (1965).

¹²S. L. Shapiro, J. A. Giordmaine, and K. W. Wecht,

Phys. Rev. Letters, **19**, 1093 (1967).

¹³G. Bret and H. P. Weber, *IEEE J. Quantum Electron.* **QE-4**, 28 (1968).

¹⁴W. Kaiser and M. Maier, *IEEE J. Quantum Electron.* **QE-4**, 67 (1968); private communication (1968).

¹⁵W. R. L. Clements and B. P. Stoicheff, *Appl. Phys. Letters* **12**, 246 (1968).

¹⁶B. P. Stoicheff, *Phys. Letters* **7**, 186 (1963); *Quantum Electronics and Coherent Light, Proceedings of the International School of Physics "Enrico Fermi," Course XXXI, 1963*, edited by C. H. Townes and P. A. Miles (Academic Press, Inc., New York, 1964), pp. 306-325.

¹⁷R. Hellwarth, *Phys. Rev.* **130**, 1850 (1963); *Current Sci. (India)* **3**, 129 (1964).

¹⁸N. Bloembergen and Y. R. Shen, *Phys. Rev.* **133**, A37 (1964); **137**, A1787 (1965).

¹⁹E. Garmire, E. Pandarese, and C. H. Townes, *Phys. Rev. Letters*, **11**, 160 (1963); R. Y. Chiao, E. Garmire, and C. H. Townes, in *Quantum Electronics and Coherent Light, Proceedings of the International School of Physics "Enrico Fermi," Course XXXI, 1963*, edited by C. H. Townes and P. A. Miles (Academic Press, Inc., New York, 1964), pp. 326-338.

²⁰P. D. Maker and R. W. Terhune, *Phys. Rev.* **137**, A801 (1965).

²¹G. Placzek in *Handbuch der Radiologie* (Akademische Verlagsgesellschaft, Leipzig, Germany, 1934), Vol. VI, Pt. 2, pp. 205-274.

²²G. Eckhardt and W. G. Wagner, *J. Mol. Spectry.* **19**, 407 (1966).

²³T. C. Damen, R. C. C. Leite, and S. P. S. Porto, *Phys. Rev. Letters* **14**, 9 (1965).

²⁴J. G. Skinner and W. G. Nilsen, *J. Opt. Soc. Am.* **58**, 113 (1968).

²⁵E. J. Stansbury, M. F. Crawford, and H. L. Welsh, *Can. J. Phys.* **31**, 954 (1953).

²⁶J. Cabannes and A. Rousset, *Compt. Rend. (Paris)* **206**, 85 (1938).

²⁷R. Y. Chiao, E. Garmire and C. H. Townes, *Phys. Rev. Letters* **13**, 479 (1964).

²⁸P. L. Kelley, *Phys. Rev. Letters*, **15**, 1005 (1965).

²⁹R. Guillien, *Physica* **3**, 895 (1963).

³⁰cf. P. V. Avizonis, K. C. Jungling, A. H. Guenther, R. M. Heimlich, and A. J. Glass, *J. Appl. Phys.* **39**, 1752 (1968).

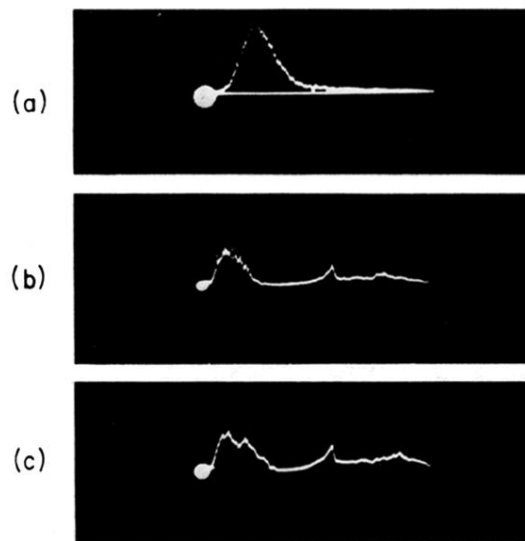
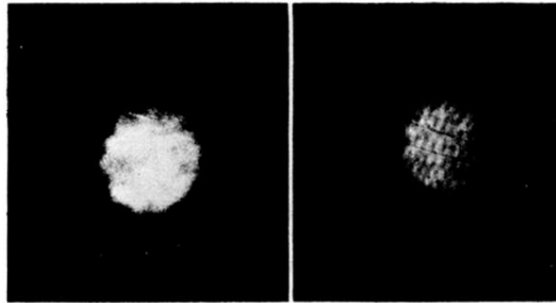


FIG. 2. (a) Typical laser pulse monitored with an ITT FW114A photodiode, and displayed on a Tektronix 519 oscilloscope. (b) Typical first-order Stokes pulse obtained in the saturation region, and the corresponding depleted laser pulse at the right. (c) Same as (b), but with the Stokes pulse also showing some depletion at higher laser power.



(a)

(b)

FIG. 3. Near-field patterns showing the spatial intensity distribution of the incident laser beam (a) and the first Stokes emission (b), magnified $20\times$. Mottled appearance of Stokes picture is caused by laser attenuating filters.